Effective electromagnetic interference shielding using polyurethane / graphite composite foam materials

Effective electromagnetic interference shielding using polyurethane / graphite composite foam materials

H Oraby[1], H R Tantawy[1], I Naeem[1], M Magdy[2], A A Ezz[3] and M Senna[4]

[1]Department of Chemical Engineering, Military Technical College, Cairo, Egypt.
[2]Department of Radar, Military Technical College, Cairo, Egypt.
[3]El-Nasr Company for Intermediate Chemicals, Industrial Area, Giza, Egypt.
[4]Radiation Chemistry Department, National Center for Radiation Research and Technology, P.O.Box 29, Nasr City, Cairo, Egypt.

E-mail: hussein.mohamed4544@yahoo.com

Abstract. Conversely, to metallic based electromagnetic interference (EMI) shielding materials; composite polymer-based foams are normally lightweight, cheaper than metals, and less sensitive to types of environmental degradation. In this work polyurethane - Graphite composite (PU-G) foam materials were prepared with different filler concentrations. Different characterization tools such as Fourier Transform Infra-Red (FTIR) and scanning electron microscope (SEM), were used to identify the structural and topological construction of the prepared composites. Further mechanical properties for the prepared samples were studied to elucidate the opportunity of utilizing these composites in applied applications, specifically for electromagnetic interference (EMI) shielding efficiency (SE) for aerospace applications. Also, in order to adjust this research in the area of aerospace EMI SE, the evaluations were executed in the X-band at (8-12) GHz. The obtained data indicated that the moreover in filler concentration enhanced the compressive strength and compressive modulus of the prepared samples. Moreover EMI SE reached -44 dB with 30 wt % graphite concentration. Finally polyurethane – graphite composite foam material can be taken into consideration a gratifying material to be utilised in EMI SE.

Keywords: electromagnetic interference; shielding; polyurethane foam; mechanical properties.

1. Introduction

The exuberant electromagnetic (EM) pollution caused by the general usage of high-frequency electronic equipment has impacted society as a whole, owing to its direct danger to human health and communication stability [1]. A system is assumed to be electromagnetically dependable with its surroundings of marginal electromagnetic interference (EMI) but, it interferes with further systems

and is not influenced by releases from additional systems [2, 3]. Decent shielding tools must also resist all received and emitted EMI [2].

Various shielding strategies were designed not only to reduce the danger of EMI but also to enhance the life time and routine of the system [4]. However, typical metal shields, particularly for aerospace applications, impose significant weight penalties [5, 6]. Due to their small weight, flimsy, low price, and processability, polymer foam composite materials (PFCM) are further desirable materials [7, 8]. PFCM have fairly large conductivities (σ) that can be easily monitored through its chemical composition [9].

Several kinds of carbon resources can be used as a conducting filler for PFCM such as graphite, carbon black, carbon fibers, carbon nanotubes, and graphene that have excellent electrical efficiency, mostly combined with polymers to protect or obstruct EM waves because of their superior properties over typical metals, such as mechanical stability, lightweight, corrosion resistance, etc… [10].

Graphite has many advantages other than carbon materials such as (1) Lower cost, (2) Doesn't need additional chemical treating, (3) Simplicity of combining with polyurethane. These composites could be turned into foams with the following advantages [11], (1) greater versatility and (2) greater EMW absorption [12].

The present study details the preparation of polyurethane – Graphite composite (PU-G) foam materials with various filler concentrations. Different characterization tools such as Fourier transform infra-red (FTIR) and scanning electron microscope (SEM), was used to identify the chemical and topological composition of the prepared composites. Further mechanical properties for the prepared samples were tested to elucidate the probability of utilizing these composites in applied applications, particularly for aerospace uses. Also, to adjust this work in the area of aerospace EMI SE, the evaluations were executed in the X-band at (8-12) GHz.

2. Theory of shielding

Proportion of remaining power to imposing power, generally equal to the overall electromagnetic (EM) waves emitted (T) by the shielding separated by the incident (i) pulse, is shielding effectiveness (SE). Electrical (E), magnetic (H) electromagnetic force (P) can be determined from any of the energy intensities:[13, 14].

$$SE = -20\log [E_T / E_i] = -20\log [H_T / H_i] = -10\log [P_T / P_i] \quad (1)$$

The EMI reduction is dependent on the wavelength, the space between the protective material and the origin of the interference, the width of the protective material and shielded content [2]. There were 3 main pathways of EM/material exchange causes SE, portion of the incident waves was redirected from the front surface of protective material, portion is taken in the shield, and portion was redirected from the rear surface, Figure 1 illustrates the mechanism of shielding efficiency. The overall efficiency of the shielding substance (SE_{Total}) is thus proportional to the sum of the absorption losses (SE_A), the reflection losses (SE_R), and the correction factor (M) for several reflections, which can be important for thin shields [15].

$$SE_{Total} = SE_A + SE_R + M \quad (2)$$

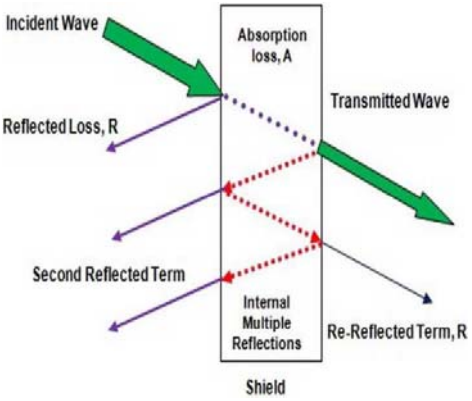

Figure 1. Mechanism of shielding efficiency

Generally, the reflection factor M was neglected at absorption loss value greater than -10 dB [13]. For simpler equations, electrical fields and plane waves can be ignored. The lack of absorption or decay takes place when currents caused in the intermediate create ohmic losses then substrate warming [16]. Reflection loss, was belonged to the relative difference between the incident wave and the protective material surface impedance. Besides, several correction factors for reflection may be negative or positive (it is usually -ve in practice) and become negligible when SE_A is > 6 dB. Usually, it is simply important by low frequencies (i.e. lower than 20 kHz) [17].

SE could be measured in two port analysis in terms of diffusion factors that detect the way voltages pass in a transmission line.

In a waveguide, as the incident EMW at a point k move to other point h, a radiated energy undergoes SE (transmission, absorption, and reflection). These wave scattering values were expressed as S_{hk}. E.g., S_{12} is the energy originating from point 2 at point 1. Thus, the S parameters S_{11} and S_{21} express the portion of redirected energy and the portion of transmitted energy, respectively [2]. The transmittance (T_{coef}), reflectance (R_{coef}), and absorbance (A_{coef}) coefficients can be expressed as follows [18, 19]:

$$T_{coef} = [E_T / E_i]^2 = S_{12}^2 = S_{21}^2 \quad (3)$$

$$R_{coef} = [E_R / E_i]^2 = S_{11}^2 = S_{22}^2 \quad (4)$$

$$A_{coef} = 1 - T_{coef} - R_{coef} \quad (5)$$

The terms A_{coef} was given here regarding the power of the EM energy. Even If the impact of various redirections among shield's two boundaries was insignificant, [20]. Positive absorbance could be well-defined as follows:

$$A_{eff} = (1 - T_{coef} - R_{coef}) / (1 - R_{coef}) \quad (6)$$

SE_A and SE_R could be defined with respect to reflectance and transmittance, respectively, by the application of power equilibrium findings [20].

$$SE_R = 10\log (1 - R_{coef}) \quad (7)$$

$$SE_A = 10\log (1 - A_{coef}) = 10\log [T_{coef} / (1 - R_{coef})] \quad (8)$$

$$SE_T = 10\log (1 - R_{coef}) + 10\log [T_{coef} / (1 - R_{coef})] \quad (9)$$

3. Experimental

3.1. Materials

For rigid PU foam formulation, the polyol mixture (with a hydroxyl number of 343.5 mg KOH g) was purchased from Alcupol R-4520 (Repsol Quimica). Methylene diphenyl diisocyanate (MDI) (Suprasec ® 5005, dark brown liquid, viscosity 220 cP at 25 ° C) was purchased from Huntsman. Graphite TPC powder (M.W: 12.01 g/mol) was obtained from CHNO, Haryana (India). All reagents were used as purchased without more treatment.

3.2. Preparation of (PU - G) composite foams

In the first step, graphite was dispersed in a polyol matrix at 5, 15 and 30 weight percent by intense sonication with an ultrasonic homogenizer for 5 min at 50 percent amplitude to achieve an identical diffusion. Polyol is carefully chosen for graphite dispersion since it is less viscous. The particulate mixture was blended with MDI in 250 ml paper cups at a ratio of 1:1.1 (polyol / MDI) in next step. For post-curing and potential research, the samples were allowed to stay at room temperature for 24 h. The prepared samples with different graphite concentration will denoted here after as follows PU, PU / G 5%, PU / G 15% and PU / G 30%.

3.3. Characterization of (PU / G) composites foam

3.3.1. FTIR spectroscopic analysis. Using a JASCO 4100 FTIR spectrometer over the 400-4100 cm^{-1} spectrum at a 5 cm^{-1} resolution, IR analysis was conducted.

3.3.2. Scanning Electron Microscopy (SEM). The topology was studied by ZEISS EVO MO-10 Germany scanning electron microscope. Samples were prepared for the SEM images of the composite foam cross-section by fracturing the related composite into liquid nitrogen.

3.3.3. Compression test. The compressive characteristics of neat PU and PU composite samples were measured with respect to ASTM D 1621-94. For the compression research, test samples with a sectional area of 25.7 cm^2 and a length of 2.53 cm were tested. For each 25.4 mm of specimen thickness, the load was applied to the sample with a crosshead movement of 2.6 mm/min. For aforementioned procedure were repeated three times for each sample and the average was approved as the final result. The compressive strength was determined automatically.

3.4. EMI SE measurements

The efficacy of the SE was calculated by ZVA-24 vector network analyzer in 8 to 12 GHz frequency. Composite foams were sliced into the aluminum waveguide sample holder into a rectangle (2.02 cm X 1.02) cm. For each foam composite, the final recorded results were the combination of three samples tested.

4. Results and Discussion

4.1 FTIR spectroscopic Analysis

The change in chemical composition structure was detected from FTIR spectra. Figure 2 displays the FT/IR spectrum of PU and PU / G 30 %. At (3427 and 3520) cm^{-1}, the pure PU foam sample showed its characteristic bands, which are due to the stretching pulsation of hydrogen bonding and (N-H) groups. At 2925 and 2865 cm^{-1}, the absorption peaks related to the symmetric and non symmetric stretching pulsation of CH_2 were detected. The bands at 1723, 1227, and 1070 cm^{-1} were belonged to carbonyl (C = O) stretch pulsation, aromatic (C-O) stretch pulsation, and (C-O-C) non symmetric stretch pulsation. At (1535 and 1225) cm^{-1}, there is a mixture of (N-H) distortion and (C-N) stretching pulsations [21]. By comparing pure PU and PU / G 30 % FTIR spectra, we can notice that the relative position of distinctive composite bands were similar to that of tidy PU foam. This suggests that the use of graphite as a filler has not changed the segmented PU foam structure, which ensures that graphite does not interact with the PU molecules [22-24].

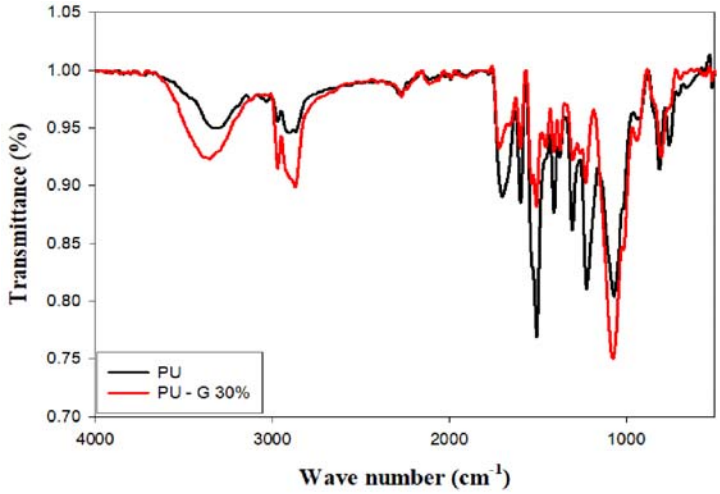

Figure 2. FTIR spectrum for PU and PU / G 30 %

4.2. Morphology of the prepared samples

The microstructure of PU, PU / G 5%, PU / G 15% and PU / G 30% foams is seen in Figure 3 (a, b, c and d). The cell was circular in the PU foam, with diameter of 315 µm. The foam cell becomes thin and irregular with the incorporation of G. The cell diameter of PU / G 5%, PU / G 15% and PU / G 30% composites, for instance, is (191, 120, and 85) µm respectively. Extra pores can be produced during the foaming phase in composite foam because of nucleation influence of G, causes reduced cell diameter [25]. Also, the great graphite/polyol mixture viscosity facilitates the joining of cells in the foaming phase, contributing to the irregular morphology of cells in composite foams. Organic materials and sonication have been usually used to prepare these foams to keep identical spreading and decrease the viscosity of the PU / G composites.

Extreme usage of organic materials, however, will cause environmental problems and more expenses, while, plentiful usage of sonication allows it more economical to manufacture large-scale nanocomposites [25].

The dispersion of graphite in polyurethane foam is shown in figure 3.d. In the polyurethane matrix, the graphite dispersion is fairly uniform but in a strongly aggregated state. The wide G agglomerates could be fragmented by the heavy shear strength produced by sonicator. Slightly aggregated G state has aided to create electrical conductive pathways [26]. Figure 3.d shows that the nucleation continues at high G content at a high rate that allows the cells to converge with each other and creates channels between cells to create an open-cell foam structure that harms the mechanical properties, and this will be addressed in the next section.

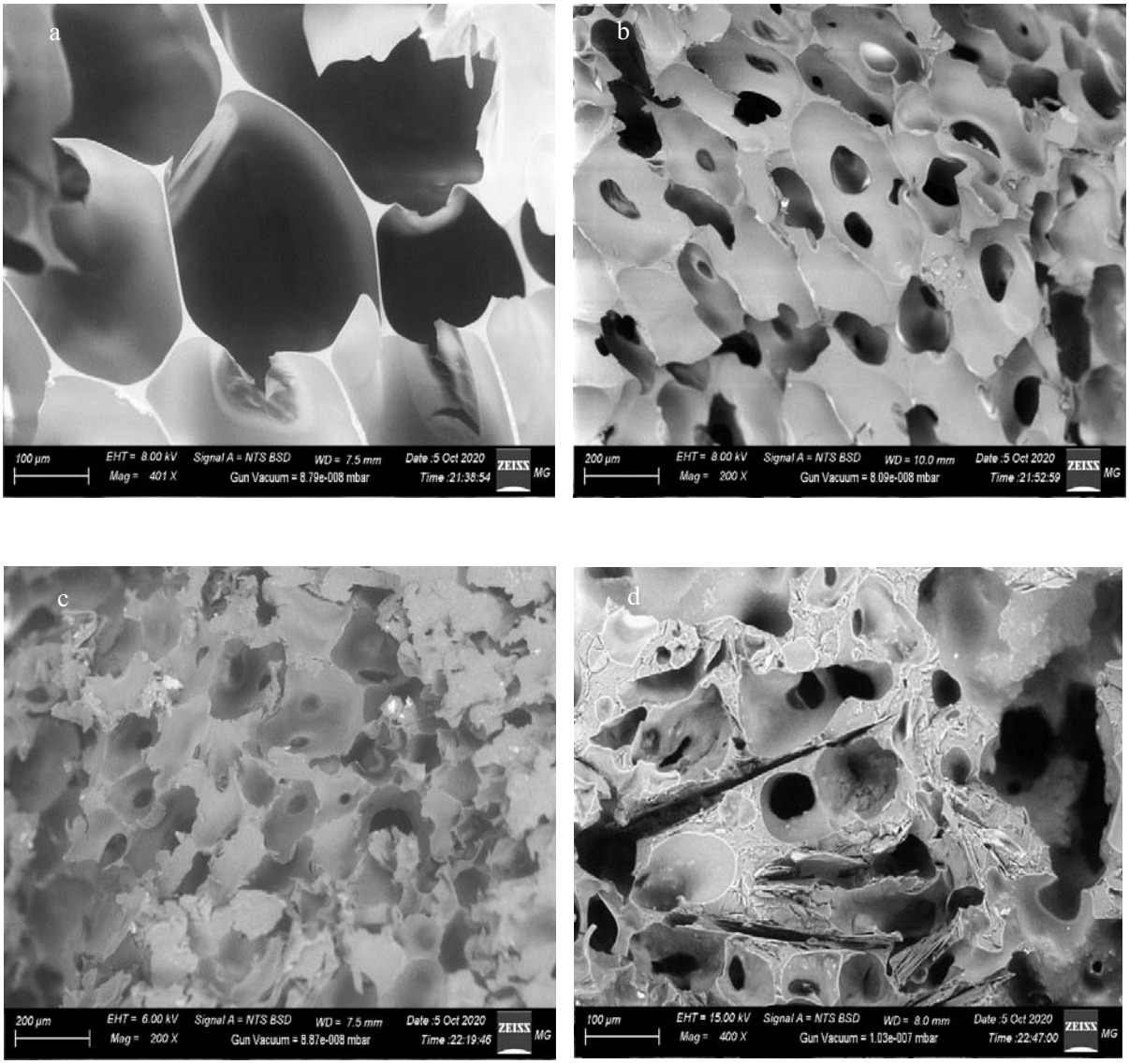

Figure 3. SEM images for a) PU, b) PU / G 5 %, c) PU / G 15 % and d) PU / G 30 %.

4.3. Mechanical compression test

Figure 4 demonstrates stress-strain curves for PU and PU-graphite composite foams. Three deformation phases were seen; original linear action, linear plateau area, and finally, densification. To estimate foam compressive modulus, the slope of the first region is used and intersection point is used to measure the compressive strength between the initial linear region and the plateau region [22]. For PU / G 5% and PU / G 15%, together compressive modulus and strength were increased, as we note that the modulus raised by 320 % and 505 % respectively and the strength also raised by 125 % and 255 %, but at 30 % concentration, the compressive module increased marginally with a rise of 3.7 % and a decrease in compressive strength of -29.7 %. We can notice that the slope of the linear plateau region is higher for all PU-G composite foams under careful observation and it is improved by increasing graphite wt percentage [22]. we can notice that the profile of the plateau region depends on structures of cells [27].

The deformation of cells happens as a merging of cells folding and collapsing in the event of a linear plateau. Therefore, the post-yield action of the PU - graphite composite foam can be enhanced until some concentration due to dispersion of graphite particles. However at higher concentrations PU-G 30% the nucleation is very strong and cell merger occurs and the foam structure becomes open cell structure with a higher percentage, thereby decreasing the mechanical properties, which confirmed by the SEM results. Table 1 summarize the compression test results.

Table 1. Compression test results

PU/G	Compressive modulus (MPa)			Compressive strength (MPa)		
	Results	Average	Gain %	Results	Average	Gain%
Neat	0.54 0.53 0.55	0.54	-	5.21 5.67 5.99	5.62	-
PU / G 5%	2.32 2.28 2.26	2.28	320 %	12.64 13.01 12.22	12.62	125 %
PU / G 15%	3.29 3.31 3.25	3.28	505 %	20.47 19.96 19.35	19.92	255 %
PU / G 30%	0.58 0.55 0.57	0.56	3.7 %	3.99 4.01 3.87	3.95	-29.7 %

4.4. Electromagnetic interference shielding effectiveness

Electromagnetic waves could be inhibited by using good shield material which could attenuates the imitating energy [28]. The shielding effectiveness for polyurethane composites with different graphite contents in the X-band frequency range (8-12) GHz is presented in Figure 5. In PU composites, SE rises with graphite percentage enrichment. A small amount of graphite containing composite PU-G 5% displayed a SE of 17 dB followed by 36 dB at PU-G 15%, and a limit of 44 dB was observed at the X-band for PU-G 30%.

As is obvious from the increasing conductivity, G particulates come to be more nearby with raising G content [28, 29]. The link of G pathways with very near gaps was formed as extra G particulates were dispersed in PU matrix which was confirmed by SEM results. Compared to PU-rich environments, these particles redirected or absorbed more radiation, causing SE value rises with higher concentration of graphite.

In this work, we find that shielding routine increases with growing frequency for samples with distinct G concentrations (5, 15, and 30) wt percent. Graphite-prepared PU composites have demonstrated relatively greater SE results rather than these synthesized for different fillers via compression molding method of melt manufacturing [30, 31]. Figure (6) shows the variance of reflection loss (RL) as a function of frequency. With the inclusion of graphite material, the highest RL value is 5.5 dB for PU / G 5% at (8-12) GHz, decreases and is found to be 3 dB for PU / G 15% and 1 dB for PU / G 30%. With frequency, it is randomly rising, and the variation for greater compositions is further disorderly. Structural properties, such as the filler scattering, through the relation of EM energy with G, may be responsible for such frequency dependency. It is obvious that PU composites with a high SE value output a smaller RL value [28].

The transmission loss variance (TL) as a function of frequency is shown in Figure 7. The minimum TL value for PU - graphite composite foam is 10 dB at PU / G 5% at (8-12) GHz, with the inclusion of graphite material, it rises to 30 dB for PU / G 15% and 40 dB for PU / G 30% is observed. We note that TL increases along the frequency spectrum, and because of the enhanced conductivity and good G scattering in PU, this variance can be called systematic [28].

Table 2 illustrates a comparison between this work and other work in literature using graphite in different polymeric matrices.

Table 2. Comparison between this work and results in the literature

No. #	Filler	Matrix	Filler	Thickness (mm)	Frequency range(GHz)	SE (dB)	ref.
1	Graphite	SEBS	20 wt%	5	8-12	-15	[32]
2	Graphite	PE	30 wt%	3	8-12	-33	[33]
3	Graphite	PE	7.5 vol%	2.5	8-12	-51.6	[34]
4	Graphite	Epoxy	2 wt%	5	8-18	-11	[35]
5	Graphite	PU	15 wt%	-	8-12	-21.7	[36]
6	Graphite	PU–Si rubber	5 wt%	-	8-12	-25	[37]
7	Graphite	PU	30 wt%	5	8-12	-44	This work
8	Graphite	PU	15 wt%	5	8-12	-35	This work

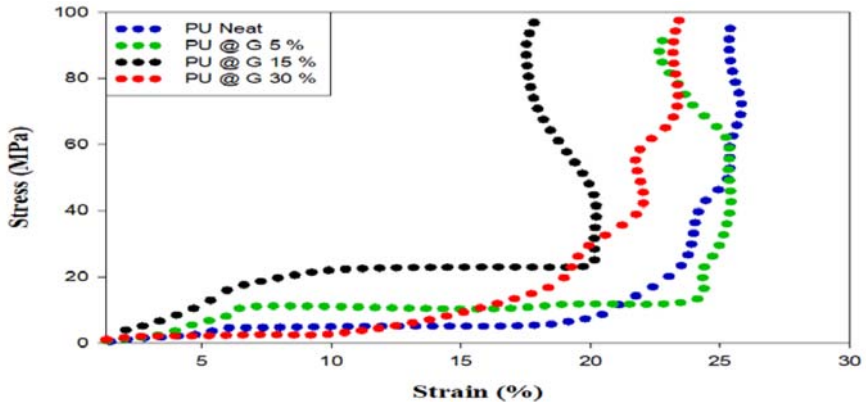

Figure 4. Compression Stress-Strain curve for a) PU, b) PU / G 5 %, c) PU / G 15 % and d) PU / G 30 %.

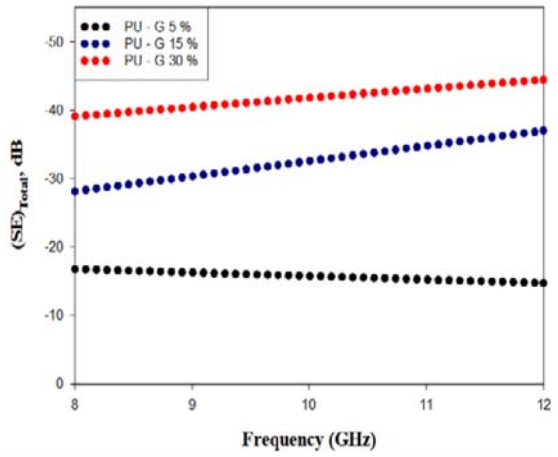

Figure 5. Total shielding efficiency (SE) as a function of graphite concentration for PU / G composite foam.

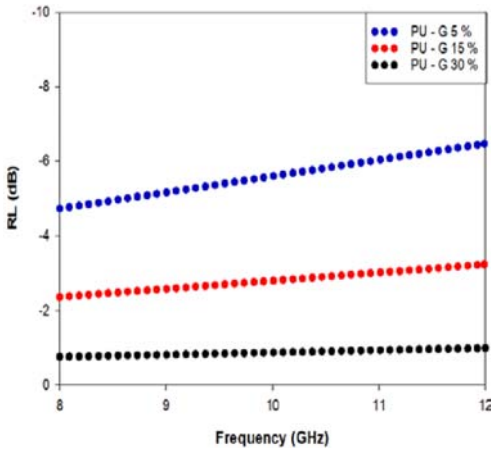

Figure 6. Reflection Loss (RL) as a function of graphite concentration for PU / G composite foam.

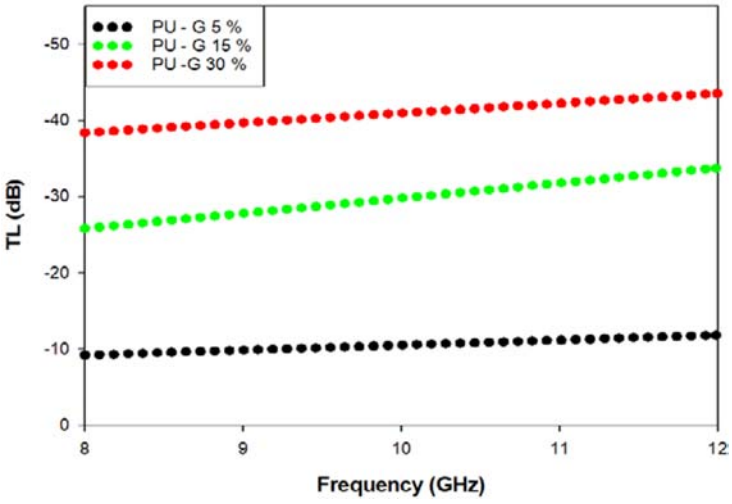

Figure 7. Transmission Loss (TL) as a function of graphite concentration for PU / G composite foam.

5. Conclusion

PU - G composite foams with great SE values were successfully prepared. SEM micrographs showed that that cell size decreases as filler concentration increases and at larger G concentration, foam construction begins to be diminished which has a negative influence on the compressive properties. Also, the mechanical properties (compressive modulus and strength) for the prepared composite foams enhanced by loading with G but, at increased G percentage the compressive characteristics weakens as SEM indicated. Also, FT/IR showed the typical bands for the prepared samples and illustrated that graphite didn't affect the PU segments structure. The prepared foam samples showed brilliant results in SE of 44 dB with PU / G 30% G

concentration. Finally, the previous results introduce an optimization between compressive characteristics and SE for PU / G samples with different concentrations. It illustrated that the optimum G % in PU foam was 15 wt % which involves the great total SE -35 dB besides an acceptable compressive properties that could be considered as a promising material in EMI SE for aerospace applications.

References

[1] Y. Li, B. Shen, D. Yi, L. Zhang, W. Zhai, X. Wei*, et al.*, 2017 "The influence of gradient and sandwich configurations on the electromagnetic interference shielding performance of multilayered thermoplastic polyurethane/graphene composite foams," *Composites Science and Technology,* vol. **138**, pp. 209-16.

[2] H. R. Tantawy, D. E. Aston, J. R. Smith, and J. L. Young, 2013 "Comparison of electromagnetic shielding with polyaniline nanopowders produced in solvent-limited conditions," *ACS applied materials & interfaces,* vol. **5**, pp. 4648-58.

[3] C. R. Paul, 2006 "*Introduction to electromagnetic compatibility"* vol. **184**: John Wiley & Sons.

[4] L. Li and D. Chung, 1991 "Electrically conducting powder filled polyimidesiloxane," *Composites,* vol. **22**, pp. 211-18.

[5] P. Liu and G.-F. Chen, 2014 "*Porous materials: processing and applications*" Elsevier.

[6] H. Nakajima, 2019 "Fabrication, Mechanical and Physical Properties, and Its Application of Lotus-Type Porous Metals," *MATERIALS TRANSACTIONS,* vol. **60**, pp. 2481-89.

[7] M. M. A. Nikje, M. A. F. Nejad, K. Shabani, and M. Haghshenas, 2013 "Preparation of magnetic polyurethane rigid foam nanocomposites," *Colloid and Polymer Science,* vol. **291**, pp. 903-9.

[8] S. Petlitckaia and A. Poulesquen, 2019 "Design of lightweight metakaolin based geopolymer foamed with hydrogen peroxide," *Ceramics International,* vol. **45**, pp. 1322-30.

[9] H. Zhang, G. Zhang, Q. Gao, M. Zong, M. Wang, and J. Qin, 2020 "Electrically electromagnetic interference shielding microcellular composite foams with 3D hierarchical graphene-carbon nanotube hybrids," *Composites Part A: Applied Science and Manufacturing,* vol. **130**, p. 105773.

[10] G. Cao, 2004 "*Nanostructures and nanomaterials: synthesis, properties and applications*" World scientific.

[11] G. Viola and W. Schmeal, 1994 "Isocyanate trimerization kinetics and heat transfer in structural reaction injection molding," *Polymer Engineering & Science,* vol. **34**, pp. 1173-86.

[12] J.-M. Thomassin, M. Trifkovic, W. Alkarmo, C. Detrembleur, C. Jérôme, and C. Macosko, 2014 "Poly (methyl methacrylate)/graphene oxide nanocomposites by a precipitation polymerization process and their dielectric and rheological characterization," *Macromolecules,* vol. **47**, pp. 2149-55.

[13] X. C. Tong, 2016 "*Advanced materials and design for electromagnetic interference shielding*" CRC press.

[14] H. S. Nalwa, 1997 "*Handbook of organic conductive molecules and polymers*" Wiley.

[15] L.-F. Chen, C. Ong, C. Neo, V. Varadan, and V. K. Varadan, 2004 "*Microwave electronics: measurement and materials characterization*" John Wiley & Sons.

[16] D. Weston, 2001 "*Electromagnetic Compatibility: Principles and Applications, Revised and Expanded*" CRC Press.

[17] J. Li, G. Zhang, Z. Ma, X. Fan, X. Fan, J. Qin*, et al.*, 2016 "Morphologies and electromagnetic interference shielding performances of microcellular epoxy/multi-wall carbon nanotube nanocomposite foams," *Composites Science and Technology,* vol. **129**, pp. 70-78.

[18] M. Verma, P. Verma, S. Dhawan, and V. Choudhary, 2015 "Tailored graphene based polyurethane composites for efficient electrostatic dissipation and electromagnetic interference shielding applications," *RSC advances,* vol. **5**, pp. 97349-58.

[19] G. Wang, G. Zhao, S. Wang, L. Zhang, and C. B. Park, 2018 "Injection-molded microcellular PLA/graphite nanocomposites with dramatically enhanced mechanical and electrical properties for ultra-efficient EMI shielding applications," *Journal of Materials Chemistry C,* vol. **6**, pp. 6847-59.
[20] B. Reddy, 2011 "*Advances in Nanocomposites: Synthesis, Characterization and Industrial Applications*" BoD–Books on Demand.
[21] J. N. Gavgani, H. Adelnia, D. Zaarei, and M. M. Gudarzi, 2016 "Lightweight flexible polyurethane/reduced ultralarge graphene oxide composite foams for electromagnetic interference shielding," *RSC advances,* vol. **6**, pp. 27517-27.
[22] M. Saha, M. E. Kabir, and S. Jeelani, 2008 "Enhancement in thermal and mechanical properties of polyurethane foam infused with nanoparticles," *Materials Science and Engineering: A,* vol. **479**, pp. 213-22.
[23] R. Seymour, G. Estes, and S. L. Cooper, 1970 "Infrared studies of segmented polyurethan elastomers. I. Hydrogen bonding," *Macromolecules,* vol. **3**, pp. 579-83.
[24] H. S. Lee, Y. K. Wang, W. J. MacKnight, and S. L. Hsu, 1988 "Spectroscopic analysis of phase-separation kinetics in model polyurethanes," *Macromolecules,* vol. **21**, pp. 270-73.
[25] T. Zhai, D. Li, G. Fei, and H. Xia, 2015 "Piezoresistive and compression resistance relaxation behavior of water blown carbon nanotube/polyurethane composite foam," *Composites Part A: Applied Science and Manufacturing,* vol. **72**, pp. 108-14.
[26] J. Aguilar, J. Bautista-Quijano, and F. Avilés, 2010 "Influence of carbon nanotube clustering on the electrical conductivity of polymer composite films," *Express Polym Lett,* vol. **4**, pp. 292-99.
[27] W. Wang, X. Liao, Y. He, J. Li, Q. Jiang, and G. Li, 2020 "Thermoplastic polyurethane/polytetrafluoroethylene composite foams with enhanced mechanical properties and anti-shrinkage capability fabricated with supercritical carbon dioxide," *The Journal of Supercritical Fluids,* p. 104861.
[28] V. Sachdev, K. Patel, S. Bhattacharya, and R. Tandon, 2011 "Electromagnetic interference shielding of graphite/acrylonitrile butadiene styrene composites," *Journal of Applied Polymer Science,* vol. **120**, pp. 1100-05.
[29] C. Y. Huang and J. F. Pai, 1997 "Studies on processing parameters and thermal stability of ENCF/ABS composites for EMI shielding," *Journal of applied polymer science,* vol. **63**, pp. 115-123.
[30] C.-Y. Huang and T.-W. Chiou, 1998 "The effect of reprocessing on the EMI shielding effectiveness of conductive fibre reinforced ABS composites," *European polymer journal,* vol. **34**, pp. 37-43.
[31] C.-Y. Huang and C.-C. Wu, 2000 "The EMI shielding effectiveness of PC/ABS/nickel-coated-carbon-fibre composites," *European polymer journal,* vol. **36**, pp. 2729-37.
[32] S. Kuester, C. Merlini, G. M. Barra, J. C. Ferreira Jr, A. Lucas, A. C. de Souza*, et al.*, 2016 "Processing and characterization of conductive composites based on poly (styrene-b-ethylene-ran-butylene-b-styrene)(SEBS) and carbon additives: A comparative study of expanded graphite and carbon black," *Composites Part B: Engineering,* vol. **84**, pp. 236-47.
[33] V. Panwar and R. Mehra, 2008 "Analysis of electrical, dielectric, and electromagnetic interference shielding behavior of graphite filled high density polyethylene composites," *Polymer Engineering & Science,* vol. **48**, pp. 2178-87.
[34] X. Jiang, D.-X. Yan, Y. Bao, H. Pang, X. Ji, and Z.-M. Li, 2015 "Facile, green and affordable strategy for structuring natural graphite/polymer composite with efficient electromagnetic interference shielding," *RSC advances,* vol. **5**, pp. 22587-92.
[35] G. De Bellis, A. Tamburrano, A. Dinescu, M. L. Santarelli, and M. S. Sarto, 2011 "Electromagnetic properties of composites containing graphite nanoplatelets at radio frequency," *Carbon,* vol. **49**, pp. 4291-300.

[36] J. M. Kim, Y. Lee, M. G. Jang, C. Han, and W. N. Kim, 2017 "Electrical conductivity and EMI shielding effectiveness of polyurethane foam–conductive filler composites," *Journal of Applied Polymer Science,* vol. **134**.
[37] J. Jeddi and A. A. Katbab, 2018 "The electrical conductivity and EMI shielding properties of polyurethane foam/*silicone* rubber/carbon black/nanographite hybrid composites," *Polymer Composites,* vol. **39**, pp. 3452-60.